Waste Engine Oil Sorption Capacity of Calcium Oxide Nanoparticle Synthesized Biologically with *Eugenia Uniflora* Leaf Extract

Felicia Uchechukwu Okwunodulu*, Stella Mbanyeaku Ufearoh and Martina Chizoba Apugo

Department of Chemistry, Michael Okpara University of Agriculture Umudike, P. M. B. Umuahia, Abia State Nigeria.

Abstract: **Biomolecules present in plant extracts can be used as capping and stabilizing agents which reduce metal ions or metal oxide ions to metal nanoparticles in a single-step green synthesis process. In this study, calcium oxide nanoparticle was synthesized using *Eugenia uniflora* leaf extract in order to ascertain its oil sorption capacity. The characterization of the calcium oxide nanoparticle through UV-vis spectroscopy revealed that maximum absorption was obtained at 207nm indicating surface plasmon absorption of calcium oxide nanoparticle. FTIR results of the *Eugenia uniflora* leaf extract before and after the synthesis of the calcium oxide nanoparticle indicated the absence of the O-H functional group of alcohol with peak at 3306.1 cm^{-1} and C-C functional group of alkane with peak at 1449.9 cm^{-1} indicating their responsibility for the reduction and capping of the synthesized calcium oxide nanoparticle. The morphology of the cacium oxide nanoparticle indicated no definite shape with smooth surface on magnification. The XRD pattern showed that the calcium oxide nanoparticle formed are crystalline in nature with average crystallite size of 3.25 to 4.76 nm. Effect of contact time on the oil sorption capacity of calcium oxide nanoparticle revealed highest sorption capacity at a shorter time (20 min). Kinetically, oil sorption capacity of CaO nanoparticle fitted the Pseudo-second-order model with R^2 close to unity (i.e. 0.996). Mechanism of sorption is by chemisorption. Therefore oil sorption capacity of calcium oxide nanoparticle proved to be effective especially at low contact time can be used to clean oil polluted water.**

Keywords: **Sorption capacity, Calcium oxide nanoparticle, *Eugenia uniflora,* Waste engine oil, Contact time.**

I. INTRODUCTION

Nanotechnology refers to an emerging field of science that includes synthesis and development of various nano-materials such as nanoparticle. Nanoparticles represent a particle with a nanometer size of 1–100 nm. The nanoscale material has new, unique, and superior physical and chemical properties compared to its bulk structure, due to an increase in the ratio of the surface area per volume of the material/particle [1]. The most widely studied nanoparticle materials are metal nanoparticles including metal oxide nanoparticles because they are easier to synthesize. Metal nanoparticles are particularly important class of nanomaterials with applications in diverse fields including electronics [2], catalysis [3] , sensing [4], water treatment [5] , oil recovery [6], corrosion inhibition [7] , drug delivery [8] , antimicrobials [9], among many others. The common inorganic nano metal oxides are magnesium oxide (MgO), titanium oxide (TiO_2), copper oxide (CuO), zinc oxide (ZnO) and calcium oxide (CaO). These nano metal oxides are safe to human and other organisms, stable, antimicrobial agents and have multifunctional properties [10]. Calcium oxide (CaO) nanoparticles have significant antimicrobial properties and unique structural and optical properties; environmentally, they are safe to all living organisms [11]. Calcium oxide nanoparticles has specific structural and optical properties, and can be used as a potential drug delivery agents in photo thermal and photodynamic therapy and synaphic delivery[12]. With potential biomedical applications, calcium oxide nanoparticles are also used in the various fields such as electronics, environmental remediation, sensors and catalysis.[13] The green synthetic approach to synthesize both metal and metal oxide nanoparticles is highly advantageous unlike the conventional method due to its minimization of hazardous chemicals, prevention of wastes, efficiency, low cost and comparatively high yield of products.[14] Various applications of bio-synthesized calcium oxide nanoparticle have been documented but none has been done on it's oil holding capacity using *Eugenia uniflora* extract. In this work, calcium oxide nanoparticles was synthesized using *Eugenia uniflora* extract. The obtained calcium oxide nanoparticle were characterized using UV-Vis spectroscopy, Fourier transform infrared (FT-IR) spectroscopy, X-ray diffraction studies (XRD), Scanning electron microscopy (SEM) techniques. Its application such as oil holding capacity was studied.

II. EXPERIMENTAL

2.1 Sample collection

The fresh leaves of *Eugenia uniflora* were collected from the *Eugenia uniflora* plant located at Nkata Ibeku in Umuahia North Local Government Area, Abia State, Nigeria and were identifed and authenticated at the taxonomy section of Forestry Department of Michael Okpara University of Agriculture Umudike Nigeria.

2.2 Preparation of aqueous leaf extract

The sliced leaves were washed properly with deionized water and then air dried at room temperature for about two weeks which were then milled into a fine powder. *Eugenia uniflora* leaves extract was prepared by weighing 100g of the fine

particles into a 1000ml glass beaker using Ataus analytical balance. 800ml of de-ionised water was added to it and stirred for some time, boiled at 80°C (in thermostatic water bath) for 15mins and was allowed to cool. The solution was filtered through Whatman No. 1. filter paper (Sprungfield MillMaidstone Kent, England) and the filtrate was used immediately for the synthesis of calcium oxide nanoparticles.

2.3 Synthesis of calcium oxide nanoparticles

25g of calcium oxide was added to 100mls of the *Eugenia Uniflora* leaves extract . The mixture was stirred using a magnetic stirrer at room temperature for 2hrs, after which 5g of the ascorbic acid was added to stabilize the zerovalent calcium oxide reduced by *Eugenia Uniflora*. The calcium oxide nanoparticle obtained was purified by repeated centrifugation at 1500 rpm for 15 mins followed by re-dispersion of the pellet in de-ionize water. Then the calcium oxide nanoparticle was dried in an oven at 80°C and then allowed to cool before storing in an airtight container for further analysis.

2.4 UV-Visible spectroscopy analysis

The bio-reduction process of calcium ions in aqueous solution was measured by sampling 1mL aliquot compared with 1 mL of de-ionized water used as blank and subsequently measuring the UV-visible spectrum of the solution. UV-visible spectrum was monitored on Cary Series UV-Visible spectrophotometer Agilent Technology, operated within the wavelength range of 200 to 800 nm.

2.5 FT-IR spectroscopy measurement

This was carried out on *Eugenia Uniflora* leaves extract and on the calcium oxide nanoparticle, FT-IR measurement of the samples was performed using FTIR-Cary 630 Fourier TransformInfrared Spectrophotometer, Agilent Technology, in a transmittance method at a resolution of 8 cm^{-1} in potassium bromide (KBr) pellets in the wave number range of 4000-650 cm^{-1}.

2.6 Scanning electron microscopy (SEM) analysis

Morphology of the nanoparticles was studied using SEM analysis with electron magnification of 80 – 150,000x (MODEL-PHENOMProX Scanning Element Microscope manufactured by Phenom World Eindhoven, Netherlands).

2.7 X-Ray diffraction (XRD) Analysis

XRD (PAN analytical, Netherlands) patterns were obtained with a diffractometer (Empyrean model, Netherrlands) operated at a voltage of 45 KV and a current of 40 mA using Cu-K radiation in a Θ-2Θ configuration with a wavelength (λ) of 1.541 Å. The sample was made smoother and was imparted on a slide which was then charged into the machine after adjusting the machine parameters and was operated via a monitor.

2.8 Oil sorption capacity

Oil sorption capacity (OHC) was calculated according [15] with slight modifications. 1g of the CaO nanoparticles powder was weighed in a pre-weighed 30mL plastic centrifuge tube. 10mls of waste motor oil was added to it and was thoroughly mixed with a vortex mixer at the highest speed and allowed to stand at room temperature (22 ± 2°C) at various time interval; 30, 60, 90, 120, 150 minutes. CaO nanoparticle-oil mixture was centrifuged at 1200 g (3500 rpm) for 30 min (Model 3K 15, motor 11133, SIGMA, Germany), the supernatant was carefully decanted and the new mass of the CaO nanoparticle was recorded. The same procedure was carried out for other time intervals. OHC (g oil / g dry CaO nanoparticle) for each time interval was calculated as:

$$\text{OHC (g oil /g powder)} = (m_{oiled} - m_d)\ /m_d \qquad 1$$

Where m_d and m_{oiled} are the mass of dry powder CaO nanoparticle and mass of dry powder CaO nanoparticle including sorbed oil, respectively. The initial weight of the sample at each time variation serves as the control analysis and the graph of OSC (g oil /g dry CaO nanoparticle) was plotted against time.

2.9 Statistical analysis

The data given in this study represents the mean of triplicate analysis. All results are evaluated by mean SD values. The correlation coefficient (R^2) values of the linear form of pseudo-first-order and pseudo-second-ordera were also determined using statistical functions of Microsoft Excel (version Office XP, Microsoft Cooperation, USA).

III. RESULTS AND DISCUSSION

3.1 UV-visible spectroscopy analysis

UV-visible spectrum of calcium oxide nanoparticle showed maximum absorption at 219nm. This is due to surface plasmon resonance (SPR) that is the resonant oscillation of conduction of electrons at the interface between negative and positive permittivity material stimulated by incident light.

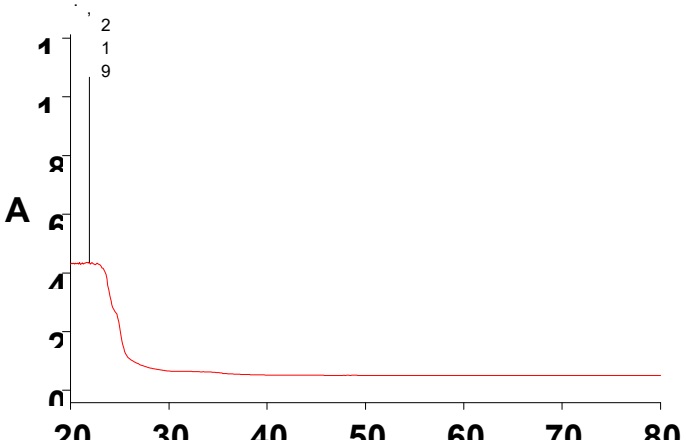

Figure 1: UV-visible spectrum of calcium oxide nanoparticle

3.2 Fourier transforms infrared spectroscopy

The FTIR analysis was carried out on *Eugenia uniflora* leaf extract and on the synthesized calcium oxide nanoparticle. FTIR measurements were used to identify the possible functional groups responsible for the reduction of calcium oxide ions to calcium oxide nanoparticle and to identify the possible biomolecules responsible for the capping and stabilization of the synthesized calcium oxide nanoparticle. Figure 2 and Table 1 show the vibrational frequencies of the functional groups present in the *Eugenia uniflora* leaf extact while Figure 3 and Table 2 show the vibrational frequencies of the functional groups present in the calcium oxide nanoparticle. From Table 1, the peaks at 3276.3 cm^{-1}, 2922.2, 2851.4 cm^{-1}, 1625.1 cm^{-1}, 1438.8 cm^{-1} and 1230.3 cm^{-1} indicated O-H of alcohol, O-H of acid, C-H of alkane, C=C of alkene or aromatic, C-C of alkane and C-O of ester or anhydride while from Table 2, the peaks at 3168.2 cm^{-1}, 2870.1 cm^{-1}, 2113.4 cm^{-1}, 1636.3 cm^{-1} and 1258.1 cm^{-1} indicated O-H of acid, C≡C of alkyne, C=C of alkene or aromatic and C-O of alcohol, ester or anhydride. The main difference in the FTIR result of the *Eugenia uniflora* leaf extract before and after the synthesis of the calcium oxide nanoparticle is indicated by the absence of the O-H functional group of alcohol with peak at 3306.1 cm-1, C-H and C-C functional group of alkane with peaks at 2851.1 cm^{-1} and 1449.9 cm^{-1} as shown in Fig. 2 which indicated that they are responsible for the capping and stabilization of the synthesized calcium oxide nanoparticles.

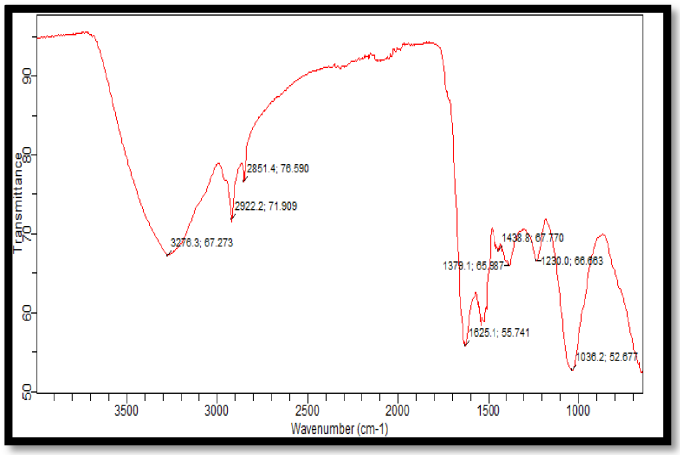

Figure 2: FTIR of Eugenia uniflora leaf extract

Table 1: Functional groups of the leaf extract of Eugenia uniflora

Peaks (wavelength in cm-1)	Functional group
3276.3	O-H of alcohol
2922.2	O-H of acid
2851.4	C-H of alkane
1625.1	C=C of alkene or aromatic
1438.8	C-C of alkane
1230.3	C-O of ester
1036.2	C-O of ester

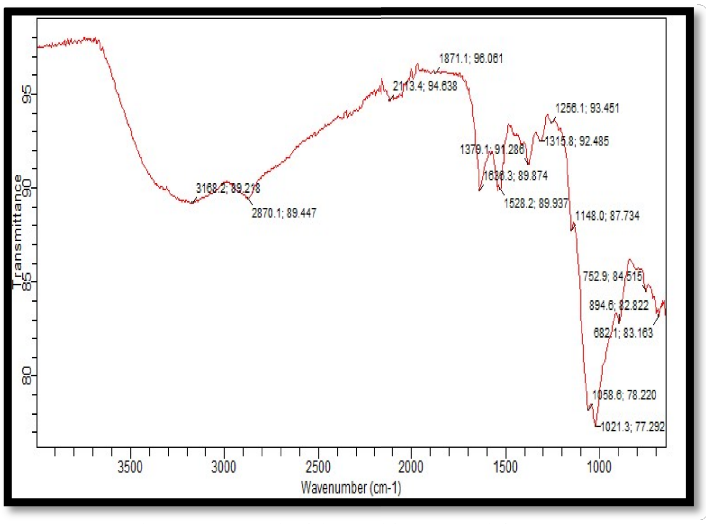

Figure 3: FTIR of calcium oxide nanoparticle .

Table 2: Functional groups of the calcium oxide nanoparticle

Peaks (wavelength in Cm-1)	Functional group
3168.2	O-H of acid
2870.1	O-H of acid
2113.4	C≡C of alkyne
1636.3	C=C of alkene or aromatic
1148	C-O of alcohol, ester or anhydride

3.3 Scanning electron microscopy analysis (SEM)

The SEM images of calcium oxide nanoparticle are shown in Fig. 4, 5, 6 and 7. The morphology of the nanoparticle indicated no definite shape of various sizes that are agglomerated. Further observations with higher magnifications reveal that these images possess smooth surfaces. At much higher magnification the images are seen as large particles which can be attributed to aggregation or clustering of smaller particles.

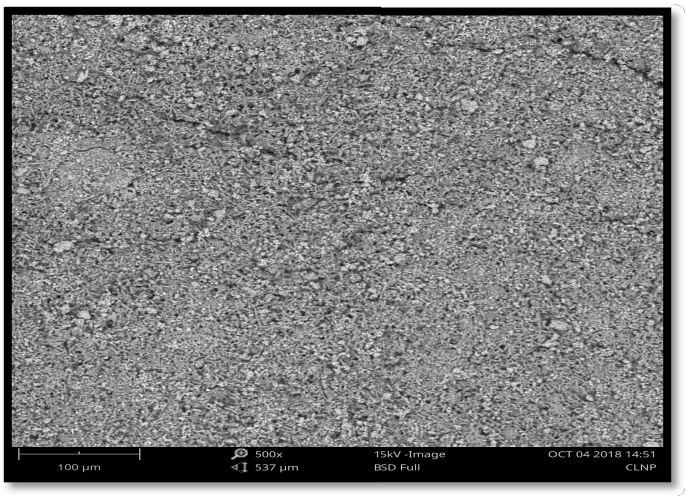

Figure 4: *SEM image of calcium oxide nanoparticle.*

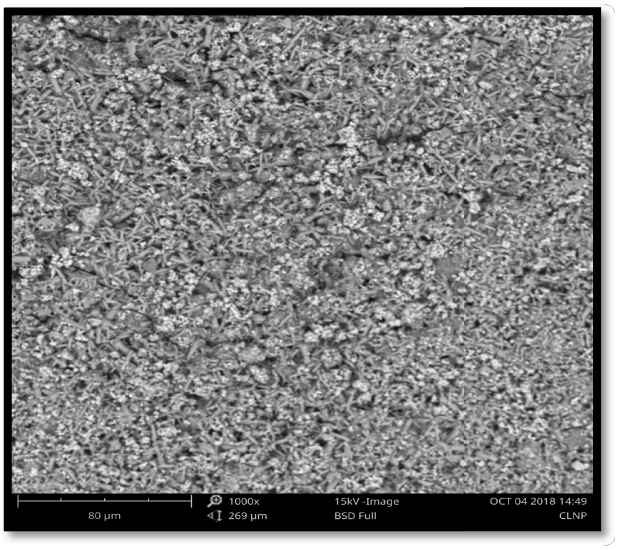

Figure 5: Zoomed SEM image of calcium oxide nanoparticle.

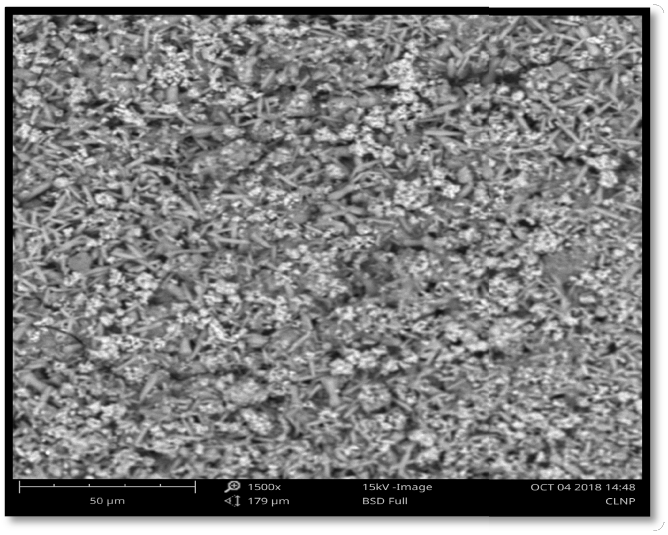

Figure 6: Zoomed SEM image of calcium oxide nanoparticle.

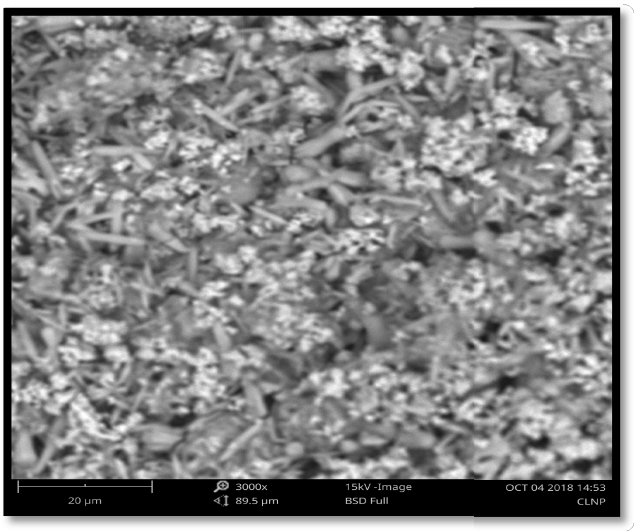

Figure 7: Zoomed SEM image of calcium oxide nanoparticle.

3.4 X-ray diffraction analysis (XRD)

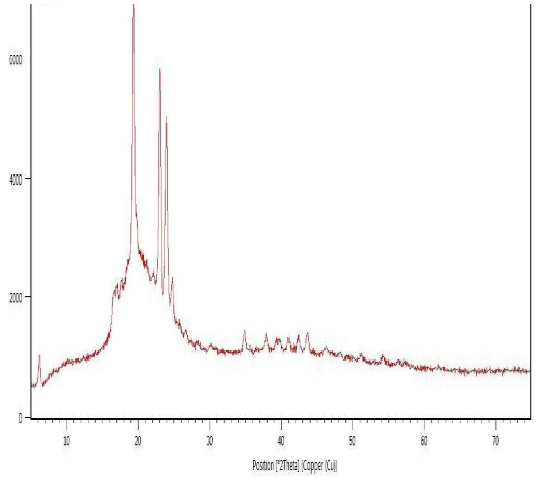

Figure 8: X-ray diffraction pattern of calcium oxide nanoparticle synthesized from Eugenia uniflora.

Figure 8 shows the XRD of calcium oxide nanoparticle biosynthesized from the leaf extract of *Eugenia uniflora*. A number of Bragg reflections values 6.23°, 19.42°, 23.05°, 23.97°, 38.87° and 43.69° within the angle range from 5.00° to 74.99°, were observed. The XRD pattern indicated that the calcium oxide nanoparticle formed are crystalline in nature with a mixed phase structure of calcium oxide nanoparticle. The average crystallite of the calcium oxide nanoparticle was calculated from the width of the XRD peaks, assuming that they are free from non-uniform strains, using the Debye-Scherrer equation shown below in equation 2.

$$D = k\lambda / \beta \cos \theta \qquad 2$$

Where D is the particle size (in nm), *k* is a constant equal to 0.94, λ is the wavelength of X-ray radiation (0.541), β is the full-width at half maximum (FWHM) of the peak (in radians) and Θ is the Bragg angle (in degrees). The average crystallite size was found to be in the range of 24 to 41 nm.

3.5 Oil sorption capacity (OSC)

Table 3: Results for the oil sorption capacity of CaO nanoparticle at various contact time

Contact time (minutes)	OSC (g oil/g CaO nanoparticle)
10	1.586±0.037
20	1.774±0.056
30	1.615±0.018
40	1.739±0.022
50	1.636±0.024
60	1.694±0.022

Table 3 shows the variation of the oil sorption capacity of the calcium oxide nanoparticle at various time intervals. From Table 3, it can be seen that the mass of oil sorbed by the calcium nanoparticle was found to increase at a shorter time (20 min) though the oil sorption capacity did not closely

follow a definite pattern which could be attributed to the quality and type of nanoparticle synthesized since the quality and type of nanoparticle synthesized using green technology are greatly influenced by length of time for which the reaction medium is incubated.[16] Similarly the characteristics of the synthesized nanoparticles can also be altered with time and are greatly influenced by the synthesis process, exposure to light, and storage conditions, and so forth.[17,18] The variations in the time may occur in many ways such as aggregation of particles due to long time storage; particles may shrink or grow during long storage; they may have shelf life, and so forth, that affects their potential.[19] From the results (Table 3), it is indicative that the amount of oil sorbed did not vary regularly with time. In some cases, the amount increases with time while in others, it decreases with time. The average impact of time on the sorption capacity of the oil depends on the number of adsorption sites available and on the strength of adsorption and desorption mechanism.

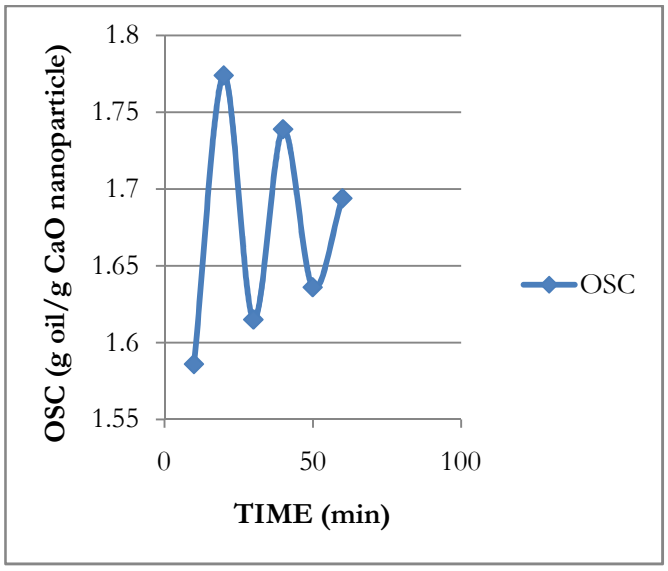

Figure 9: Graph showing plots for the holding capacity of CaO nanoparticle versus contact time.

3.6 Kinetic studies:

Several kinetic models including pseudo-first-order, pseudo-second-order and intra-particle diffusion models are common kinetic models that can be used to examine the controlling mechanism involved in the sorption of oil by the CaO nanoparticle.

The pseudo-first-order equation is given as [20]:

$$\log (q_e - q_t) = \log(q_e) - k_1 t/2.303 \qquad 3$$

where q_e and q_t are the amount of oil sorbed at equilibrium and at time, t (respectively g/g) and k_1 is the first-order rate constant (min^{-1}). From equation 3, a plot of $\log(q_e - q_t)$ versus t should be linear if a pseudo-first-order kinetic is obeyed. However, when sorption data obtained for the oil was fitted into the model expressed by equation 2, values of R^2 obtained from the plots (plots not shown) were very low indicating that the sorption of oil by the CaO nanoparticle is not consistent with a pseudo-first-order kinetics.

According to [21], a pseudo-second-order sorption rate equation can be expressed as follows,

$$dq_t/d_t = k_2 (q_e - q_t)^2 \qquad 4$$

where k_2 is the rate constant of pseudo-second-order sorption ($gmg^{-1}min^{-1}$), q_e and q_t are the sorption capacity at equilibrium and at time, t, respectively. Introducing boundary conditions to equation 4, i.e t = 0 to t=t and q_e = 0 to q_t = q_t, integrated form of equation 4 was obtained (equation 5) and upon simplification, equations 6 and 7 were obtained.

$$1/(q_e - q_t) = 1/q_e + k_2 t \qquad 5$$

$$1/q_t = 1/k_2 q_e^2 + 1/q_e(t) \qquad 6$$

$$1/q_t = 1/h + 1/q_e (t) \qquad 7$$

The implication of equation 7 is that a plot of t/q_t versus t should be linear with slope and intercept equal to q_e and $\frac{1}{h}$ ($h = k_2 q_e^2$) respectively. Fig. 9 shows a pseudo-second-order kinetic plots for the adsorption of oil by CaO nanoparticle. Sorption parameters obtained from the plots are presented in Table 4. From the results obtained, it can be seen that values of R^2 are very close to unity indicating the application of a pseudo-second-order model to the sorption of oil by the CaO nanoparticle. It is also evident from the results that the values of k_2 and h calculated from the plots are not relatively low. The value of q_e from the plot is almost equal to the equilibrium sorption capacity indicating fitness of pseudo-second-order model which is based on the assumption that the rate limiting step may be chemical adsorption involving valence forces through sharing or exchange of elections between the absorbent and adsorbate.

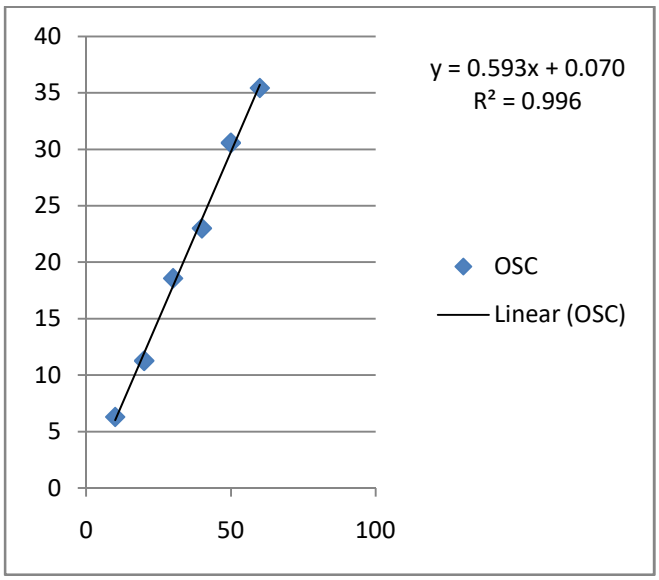

Figure 9: Pseudo-second-order kinetic plots for the sorption of oil by CaO nanoparticle.

Table 4: Pseudo-second-order sorption parameters for the sorption of oil by CaO nanoparticles

q_e(g/g)	K_2	h_o	R^2
1.6863	0.5024	1.4287	0.9960

IV. CONCLUSIONS

Characteristics of calcium oxide nanoparticle via UV-Visible, FTIR, SEM, XRD revealed maximum absorption at 207nm which is a very good indication for surface Plasmon absorption of calcium oxide nanoparticle. Different functional groups where observed in both the leave extract of *Eugenia uniflora* and calcium oxide nanoparticle synthesized with the *Eugenia uniflora*, and it was deduced that some of the functional groups observed in a leaf extract did not appeared in the calcium oxide nanoparticle indicating their usage in the formation of calcium oxide nanoparticle. The morphology of the nanoparticle indicated no definite shape of various sizes that are agglomerated. Further observations with higher magnifications revealed smooth surfaces of the images. At much higher magnification the images are seen as large particles which can be attributed to aggregation or clustering of smaller particles. The average crystalline size was found to be in the range of 3.25 to 4.76nm indicating that the calcium nanoparticle is within the nanoparticle. Oil sorption capacity of CaO nanoparticle was found to be affected by an operational variation such as contact time which proved to be very effective especially at low contact time. The mechanism of sorption is by chemisorption. Kinetically, oil sorption capacity of CaO nanoparticle fitted the Pseudo-second-order model. Therefore CaO nanoparticle can be used to clean oil polluted water.

CONFLICT OF INTEREST

There is no conflict of interest to declare

ACKNOWLEDGEMENTS

The authors acknowledge access to the facilities in the Ahmadu Bello University Nigeria for UV-vis, SEM, IR and XRD analysis and the assistance of Mr Nwadinobi Solomon in the Department of Chemistry, Michael Okpara University of Agriculture Umudike Nigeria for the oil sorption analysis.

REFERENCES

[1] B. L. Cushing, V. L. Kolesnichenko and C. J. O. Connor, "Recent advances in the liquid-phase syntheses of inorganic nanoparticles," Chemical Reviews, vol. 104, no. 9, pp. 3893–3946, 2004. https://doi.org/10.1021/cr030027b

[2] K. Shoueir, H. El-Sheshtawy, M. Misbah, H. El-hosainy, I. El-mehasseb and M. El-Kemary, "Fenton-like nanocatalyst for photodegradation of methylene blue under visible light activated by hybrid green DNSA@Chitosan@$MnFe_2O_4$", Carbohydrate Polymers, , vol. 197, pp. 17-28, 2018. https://doi.org/10.1016/j.carbpol.2018.05.076

[3] A. Mezni , M. M. Ibrahim , M. El-Kemary , A. A. Shaltout , N. Y. Mostafa , J. Ryl and M. A. Amin , "Cathodically activated Au/TiO_2 nanocomposite synthesized by a new facile solvothermal method: An efficient electrocatalyst with Pt-like activity for hydrogen generation," *Electrochim. Acta*, vol. 290, pp. 404-418, 2018. .DOI: https://doi.org/10.1016/j.electacta.2018.08.083

[4] H. Hapuarachchi, S. Mallawaarachchi, H. T Hattori, W. Zhu and M. Premaratne, "Optoelectronic figure of merit of a metal nanoparticle—quantum dot (MNP-QD) hybrid molecule for assessing its suitability for sensing applications," Journal of Physics: Condensed Matter, vol. 30, no. 5, pp. 4006, 2018. DOI: https://doi.org/10.1088/1361-648X/aaa46d

[5] K. Salama, R. Shoueir and H. A. Aljohani, "Preparation of sustainable nanocomposite as new adsorbent for dyes removal," *Fibers Polym.,* vol. 18, no. 9, 1825-1830, 2017. DOI: https://doi.org/10.1007/s12221-017-7396-0

[6] J. S. Nworu and J. O. Wilberforce Oti, "Application of Nanotechnology for Enhancing Oil Recovery (EOR) in Oil and Gas Industry: A Review," IOSR Journal of Applied Chemistry, vol. 12, no. 2, pp. 32-42, 2019. DOI: 10.9790/5736-1202023242

[7] M. M. Solomon, H. Gerengi, S. A.Umoren, N. B. Essien, U. B. Essien and E. Kaya," Gum Arabic-silver nanoparticles composite as a green anticorrosive formulation for steel corrosion in strong acid media," Carbohydrate Polymers**,** vol. 181, pp. 43-55, 2018. https://doi.org/10.1016/j.carbpol.2017.10.051

[8] E. Mona, B. Kalaivani, S. Bullo, F. Sharida and Z. H. Mohd, "The Impact of Magnesium–Aluminum-Layered Double Hydroxide-Based Polyvinyl Alcohol Coated on Magnetite on the Preparation of Core-Shell Nanoparticles as a Drug Delivery Agent," International Journal of Molecular Sciences, vol. 20, no. 15, pp. 3764, 2019. DOI: 10.3390/ijms20153764

[9] E. Sánchez-López, D. Gomes, G. Esteruelas, L. Bonilla, A. L. Lopez-Machado, R. Galindo, A. Cano, M. Espina, M. Ettcheto, A. Camins, A. M. Silva, A. Durazzo, A. Santini, M. L. Garcia, and E. B. Souto, "Metal-Based Nanoparticles as Antimicrobial Agents: An Overview" Nanomaterials (Basel).,Vol. 10, no. 2, pp. 292, 2020. . DOI: 10.3390/nano10020292

[10] B. Ramola, N. Chandra Joshi, M. Ramola, J. Chhabra and A. Singh, "Green Synthesis, Characterisations and Antimicrobial Activities of CaO Nanoparticles," Oriental Journal of Chemistry vol. 35, no. 3, 2019. DOI **:** http://dx.doi.org/10.13005/ojc/350333

[11] B. Ramola, N. Chandra Joshi, M. Ramola, J. Chhabra and A. Singh, "Green Synthesis, Characterisations and Antimicrobial Activities of CaO Nanoparticles," Oriental Journal of Chemistry vol. 35, no. 3, 2019. DOI **:** http://dx.doi.org/10.13005/ojc/350333

[12] S. Abraham and V. P. Sarathy, "Biomedical applications of calcium oxide nanoparticles – a spectroscopic study," *Int. J. Pharm. Sci. Rev. Res*., vol. 49, pp. 121-125, 2018. www.globalresearchonline.ne

[13] A. S. Balaganesh, R. Sengodan, R. Ranjithkumar and B. Chandarshekar, "Synthesis and Characterization of Porous Calcium Oxide Nanoparticles (CaO NPS), "International J. of Innov. Techn. Expl. Engin., vol. 8, no. 2, pp. 312-314, 2018. Website: **www.ijitee.org**

[14] S. Jagpreet, D. Tanushree, K. Ki-Hyun, R. Mohit, S. Pallabi and K. Pawan, "Green synthesis of metals and their oxide nanoparticles: applications for environmental remediation," J. Nanobiotechnology, vol. 16, no. 1, pp. 84, 2018. DOI: 10.1186/s12951-018-0408-4

[15] Y. Song, W. Su and Y. Chun Mu, "Modification of bamboo shoot dietary fiber by extrusion-cellulase technology and its properties,"International Journal of Food Properties, vol. 21, no. 1, pp. 1219-1232, 2018.https://doi.org/10.1080/10942912.2018.1479715

[16] A. Datta, C. Patra, H. Bharadwaj, S. Kaur, N. Dimri and R. Khajuria, "Green synthesis of zinc oxide nanoparticles using parthenium hysterophorus leaf extract and evaluation of their antibacterial properties," Journal of Biotechnology and Biomaterials, vol. 7, pp. 271 – 275, 2017. DOI: 10.4172/2155-952X.1000271.

[17] S. V. N. T. Kuchibhatla, A. S. Karakoti, D. R. Baer and S. K. Samudraia, "Influence of aging and environment on nanoparticle chemistry: Implication to confinement effects in nanoceria," Journal of Physical Chemistry *C*, vol. 116, no. 26, pp. 14108–14114, 2012. DOI: 10.1021/jp300725s

[18] I. A. Mudunkotuwa, J. M. Pettibone and V. H. Grassian,

"Environmental implications of nanoparticle aging in the processing and fate of copper-based nanomaterials," Environmental Science and Technology, vol. 46, no. 13, PP. 7001–7010, 2012. https://doi.org/10.1021/es203851d

[19] R. Baer, "Surface characterization of nanoparticles: critical needs and significant challenges," Journal of Surface Analysis, vol. 17, no. 3, pp. 163–169 2011. DOI: 10.1384/jsa.17.163

[20] Y. A. Yahaya, M. M. Don and S. Bhatia, Biosorption of Cu(II) ions onto immobilized cells of *Pycnoporous sanguineus* from aqueous solution: Equillibrium and kinetic studies, Journal of Harzadous Materials, vol. 161, pp. 189–195, 2009. DOI: 10.1016/j.jhazmat.2008.03.104

[21] Y. S. Ho, G. Mckay, D. A. J. Wase and C. F. Forster," Study of the sorption of divalent metal ions onto peat," Adsorp. Sci. Technol., vol. 18, no. 7, pp. 639 –650, 2000. https://doi.org/10.1260/0263617001493693